THE JOURNAL OF BIOLOGICAL CHEMISTRY VOL. 282, NO. 6, pp. 3640–3652, February 9, 2007

A Potential Role for Multiple Tissue Kallikrein Serine Proteases in Epidermal Desquamation*

Received for publication, August 8, 2006, and in revised form, December 4, 2006 Published, JBC Papers in Press, December 11, 2006, DOI 10.1074/jbc.M607567200

Carla A. Borgoño[‡], Iacovos P. Michael[‡], Nahoko Komatsu[‡], Arumugam Jayakumar[§], Ravi Kapadia[§], Gary L. Clayman[§¶], Georgia Sotiropoulou[‖], and Eleftherios P. Diamandis[‡1]

From the [‡]Department of Pathology and Laboratory Medicine, Mount Sinai Hospital and the Department of Laboratory Medicine and Pathobiology, University of Toronto, Toronto, Ontario M5G 1X5, Canada, the [§]Department of Head and Neck Surgery and [¶]Department of Cancer Biology, University of Texas M. D. Anderson Cancer Center, Houston, Texas 77030-4095, and the [‖]Department of Pharmacy, School of Health Sciences, University of Patras, Rion, 26500 Patras, Greece

Desquamation of the stratum corneum is a serine protease-dependent process. Two members of the human tissue kallikrein (KLK) family of (chymo)tryptic-like serine proteases, KLK5 and KLK7, are implicated in desquamation by digestion of (corneo)desmosomes and inhibition by desquamation-related serine protease inhibitors (SPIs). However, the epidermal localization and specificity of additional KLKs also supports a role for these enzymes in desquamation. This study aims to delineate the probable contribution of KLK1, KLK5, KLK6, KLK13, and KLK14 to desquamation by examining their interactions, *in vitro*, with: 1) colocalized SPI, lympho-epithelial Kazal-type-related inhibitor (LEKTI, four recombinant fragments containing inhibitory domains 1–6 (rLEKTI(1–6)), domains 6–8 and partial domain 9 (rLEKTI(6–9′)), domains 9–12 (rLEKTI(9–12)), and domains 12–15 (rLEKTI(12–15)), secretory leukocyte protease inhibitor, and elafin and 2) their ability to digest the (corneo)desmosomal cadherin, desmoglein 1. KLK1 was not inhibited by any SPI tested. KLK5, KLK6, KLK13, and KLK14 were potently inhibited by rLEKTI(1–6), rLEKTI(6–9′), and rLEKTI(9–12) with K_i values in the range of 2.3–28.4 nM, 6.1–221 nM, and 2.7–416 nM for each respective fragment. Only KLK5 was inhibited by rLEKTI(12–15) (K_i = 21.8 nM). No KLK was inhibited by secretory leukocyte protease inhibitor or elafin. Apart from KLK13, all KLKs digested the ectodomain of desmoglein 1 within cadherin repeats, Ca^{2+} binding sites, or in the juxtamembrane region. Our study indicates that multiple KLKs may participate in desquamation through cleavage of desmoglein 1 and regulation by LEKTI. These findings may have clinical implications for the treatment of skin disorders in which KLK activity is elevated.

As the outermost layer of the skin, the stratum corneum functions as the body's main protective barrier against physical and chemical damage, dehydration, and microbial pathogens. Inter-corneocyte cohesion within the stratum corneum depends primarily on corneodesmosomes, structurally modified desmosomes (1–3). Akin to classical desmosomes, corneodesmosomes maintain tissue integrity and mediate cell adhesion via calcium-dependent interactions between two families of desmosomal cadherins, the desmogleins (DSG1–4)[2] and desmocollins 1–3 (4, 5). The most abundant isoforms in the stratum corneum include DSG1, DSG4, and desmocollin-1 (6, 7). As specialized desmosomes, corneodesmosomes also contain a unique glycoprotein constituent, corneodesmosin (3).

During normal stratum corneum desquamation, the most superficial corneocytes are shed from the skin surface. This process requires proteolysis of the corneodesmosomal adhesion molecules DSG1 (8, 9), desmocollin-1 (10), and corneodesmosin (11) likely mediated by both trypsin-like and chymotrypsin-like serine proteases (9, 12). To date, serine protease activity in the stratum corneum has been attributed to human tissue kallikreins (KLK; encoded by *KLK* genes (EC 3.4.21)), a subgroup of 15 secreted serine proteases with (chymo)trypsin-like specificity (13). Among KLKs, a role in stratum corneum desquamation has been ascribed to KLK5 and KLK7, originally denoted stratum corneum tryptic enzyme (14, 15) and stratum corneum chymotryptic enzyme (16–18), respectively. Both enzymes are maximally expressed in the stratum granulosum (15, 19, 20) and transported to stratum corneum interstices by lamellar granules (20–22), where they are thought to form a proteolytic cascade in which KLK5 activates itself and KLK7 (23). Once active, both enzymes have been shown to concertedly digest DSG1, desmocollin-1, and corneodesmosin, *in vitro* (11, 24, 25).

In addition to KLKs 5 and 7, accumulating reports suggest that other kallikreins are candidate desquamation-related enzymes, based on their epidermal localization and substrate specificity. For instance, kallikrein 1, 4, 6, 8, 9, 10, 11, 13, and 14 transcripts and/or proteins are also expressed in the stratum granulosum (26–28), and kallikrein 6, 8, 10, 11, 13, and 14 protein levels have been quantified in the stratum corneum (29). Interestingly, Stefansson *et al.* (30) have recently shown that

* The costs of publication of this article were defrayed in part by the payment of page charges. This article must therefore be hereby marked "*advertisement*" in accordance with 18 U.S.C. Section 1734 solely to indicate this fact.

[1] To whom correspondence should be addressed: Dept. of Pathology and Laboratory Medicine, Mount Sinai Hospital, 600 University Ave., Toronto, Ontario M5G 1X5, Canada. Tel.: 416-586-8443; Fax: 416-586-8628; E-mail: ediamandis@mtsinai.on.ca.

[2] The abbreviations used are: DSG, desmoglein; *KLK*, human tissue kallikrein gene; KLK, human tissue kallikrein protein; LEKTI, lymphoepithelial Kazal-type related inhibitor; NE, neutrophil elastase; NS, Netherton syndrome; SKALP, skin-derived antileukoproteinase; SLPI, secretory leukocyte proteinase inhibitor; SPI, serine protease inhibitor; *SPINK5*, serine protease inhibitor kazal-type 5; TBS-T, Tris-buffered saline-Tween; WAP, whey acid protein; trappin, transglutaminase substrate and wap domain containing protein; AMC, 7-Amino-4-methylcoumarin; Boc, *t*-butoxycarbonyl; Bis-Tris, 2-[bis(2-hydroxyethyl)amino]-2-(hydroxymethyl)propane-1,3-diol.

KLK14 is responsible for ~50% of the total trypsin-like serine protease activity in the stratum corneum. Moreover, because KLK14 can activate and be activated by KLK5, it may also participate in the cascade pathway (23).

Because desquamation is a serine protease-dependent process (9, 12), it is regulated by serine protease inhibitors (SPIs). The serine protease/SPI balance governing desquamation is best illustrated by its imbalance in Netherton syndrome (NS; OMIM 256500) (31–33). NS, an autosomal recessive ichthyotic skin disorder characterized by hair shaft defects, atopic features, overdesquamation of corneocytes, and severe stratum corneum barrier dysfunction (31, 34), is caused by frameshift and nonsense mutations in the serine protease inhibitor Kazal-type 5 (*SPINK5*) gene (31, 35, 36). *SPINK5* codes for an SPI with 15 inhibitory domains, which is denoted lympho-epithelial Kazal-type related inhibitor (LEKTI) (37). All *SPINK5* mutations introduce premature termination codons in LEKTI transcripts and lead to the production of truncated LEKTI forms that lack several inhibitory domains (35, 36). Consequently, the decrease in LEKTI expression/activity in NS causes unrestricted, elevated serine protease activity, as observed in the stratum corneum of NS patients (25, 31, 33) and of *Spink5*$^{-/-}$ mice (32), leading to overdesquamation and stratum corneum thinning. The predicted activity of LEKTI against trypsin-like serine proteases based on the predominance of basic P1 residues within its inhibitory domains, the colocalization of LEKTI with multiple trypsin-like kallikrein serine proteases within the stratum granulosum and stratum corneum (22, 31, 33, 38), and the ability of LEKTI (domains 6, 6–9′, and 9–12) to inhibit KLK5 and KLK7 *in vitro* (39, 40), strongly suggest that KLKs are *in vivo* LEKTI targets and further substantiate the role of KLKs as desquamatory enzymes. In addition to LEKTI, the skin contains other SPIs that may regulate desquamation and KLK activity. KLK7 is inhibited by two members of the trappin (transglutaminase substrate and wap (whey acid protein) domain containing protein) gene family, namely secretory leukocyte protease inhibitor (SLPI; also known as antileukoprotease) and elafin (also referred to as proteinase inhibitor 3 and skin-derived antileukoprotease (SKALP)) (41) as well as a novel member of the α_2-macroglobulin family, α_2-macroglobulin-like-1 (42).

Although the (chymo)trypsin-like substrate specificity and epidermal localization of many KLKs other than KLK5 and KLK7 are compatible with a function in the terminal stages of epidermal turnover, their role as desquamatory proteases has not been investigated. Thus, in an attempt to delineate the possible involvement of multiple KLKs in desquamation, this study examines the interactions between KLK1, KLK5, KLK6, KLK13, and KLK14 with: 1) epidermal SPI (LEKTI, SLPI, and elafin/SKALP) and 2) the (corneo)desmosomal cadherin DSG1, *in vitro*.

EXPERIMENTAL PROCEDURES

Materials—7-Amino-4-methylcoumarin (AMC) was purchased from Sigma-Aldrich. AMC peptide substrates Boc-Val-Pro-Arg-AMC (VPR-AMC), H-Pro-Phe-Arg-AMC (PFR-AMC), and Boc-Gln-Ala-Arg-AMC (QAR-AMC) were purchased from Bachem Bioscience (King of Prussia, PA), and methoxysuccinyl-Ala-Ala-Pro-Val-AMC (AAPV-AMC) was obtained from Calbiochem. All substrates were diluted to a final concentration of 80 mM in Me_2SO and stored at −20 °C. Recombinant mature KLK1 and KLK6 were expressed and purified from a baculovirus/insect cell line system as previously described (43, 44) (kind gifts from Dr. M. Blaber, Florida State University). Recombinant pro-KLK5, pro-KLK13, and mature KLK14 were produced using the Easyselect™ *Pichia pastoris* expression system (Invitrogen) as described in detail elsewhere (45–47). KLKs were purified to homogeneity (>95% purity on Coomassie Blue-stained polyacrylamide gels), and their identities were confirmed by tandem mass spectrometry. Recombinant LEKTI fragments containing intact domains 1–6 (rLEKTI(1–6)), domains 6–8 and partial domain 9 (rLEKTI(6–9′)), domains 9–12 (rLEKTI(9–12)), and domains 12–15 (rLEKTI(12–15)) were produced in a baculovirus/insect cell line system as previously reported (40, 48–50). Recombinant neutrophil elastase (NE) and elafin were purchased from Calbiochem and Sigma-Aldrich, respectively, diluted in water to a final concentration of 0.5 g/liter, and stored at −80 °C. Recombinant SLPI and a recombinant DSG1/Fc chimera were obtained from R&D Systems Inc. (Minneapolis, MN), reconstituted in phosphate-buffered saline (pH 7.4) to final concentrations of 0.5 g/liter and 0.25 g/liter, respectively, and stored at −80 °C. Anti-LEKTI monoclonal antibodies 1C11G6 and 1D6G8 were produced as previously described (50).

Kinetic Inhibition Assays—The putative inhibitory effect of LEKTI domains 1–6, 6–9′, 9–12, and 12–15, SLPI, and elafin on multiple KLKs was assessed by measuring residual protease activity against AMC peptide substrates after incubation with individual inhibitors. The inhibition of NE by SLPI and elafin was used as a positive control. Assays were performed using optimal substrates (PFR-AMC for KLK1; VPR-AMC for KLK5, KLK6, and KLK13; QAR-AMC for KLK14; and AAPV-AMC for NE) and buffer conditions (KLK1: 0.1 M Tris-HCl, 0.1 M NaCl, 0.01% Tween-20, pH 8.0; KLK5, KLK13, and KLK14: 0.1 M sodium phosphate, 0.01% Tween 20, pH 8.0; KLK6: 50 mM Tris, 0.1 M NaCl, 0.2% bovine serum albumin, pH 7.3; and neutrophil elastase: 0.2 M Tris-HCl, 0.01% Tween-20, pH 7.5) (45, 51–54).

Proteases (final concentration of 12 nM for KLK1, KLK5, KLK13, KLK14, and NE or 30 nM for KLK6) were preincubated with LEKTI fragments (0–60 nM), SLPI (0–1.2 μM), and/or elafin (0–1.2 μM) in 10 μl of optimal buffer at 25 °C (for LEKTI reactions) or 37 °C (for SLPI and elafin reactions) with gentle agitation for different time points (10 min for KLK1 and KLK6, 5 min for KLK6, 1 min for KLK5, and 10 s for KLK14 with LEKTI fragments; 30 min for KLK1, KLK6, and KLK13, 5 min for KLK6 and KLK14, and 1 min for NE with SLPI and elafin). The mixtures were subsequently added to 90 μl of optimal buffer containing several fixed AMC peptide concentrations ranging from 4 to 3000 μM within polystyrene microtiter plate wells. Initial rates of protease-mediated peptide hydrolysis were monitored by measuring free AMC fluorescence on the Wallac 1420 Victor^{2TM} fluorometer (PerkinElmer Life Sciences) with excitation and emission filters of 380 and 480 nm, respectively, at 1-min intervals for 20 min at 37 °C. Protease-free reactions, for each substrate concentration, were used as negative con-

trols, and the background counts obtained were subtracted from each value. A standard curve was constructed using known concentrations of AMC to convert rates of reaction from AMC fluorescence counts/min to free AMC produced/min. The slope of the resultant AMC standard curve was 19.184 AMC fluorescence counts/nM AMC.

The rate changes (nanomolar AMC/min) of inhibited and control reactions were determined from the velocity plots. Activities were expressed relative to control incubations from which inhibitors were excluded. Average IC_{50} values, *i.e.* the inhibitor concentration required for 50% inhibition of protease activity, were determined by non-linear regression analysis using Prism (Version 4.0, GraphPad, San Diego, CA). Michaelis-Menten parameters (K_m and V_{max}), the equilibrium inhibition constant (K_i), and inhibitory mechanisms were determined by linear and non-linear regression analysis using the Enzyme Kinetics Module 1.1 (Sigma Plot, SSPS, Chicago, IL). All experiments were performed in triplicate and repeated at least twice.

In Vitro Digestion of LEKTI and SLPI by KLKs—LEKTI (10 ng) or SLPI (500 ng) were incubated separately with KLK1, KLK5, KLK6, KLK13, and KLK14 (1 ng for LEKTI reactions; 50 ng for SLPI reactions) in a final optimal buffer volume of 20 μl for different time points ranging from 0 to 24 h at 37 °C with shaking. Control reactions, *i.e.* KLKs, LEKTI, and SLPI incubated alone, were also performed. Reactions were terminated by freezing in liquid nitrogen and were subsequently resolved by SDS-PAGE using the NuPAGE Bis-Tris electrophoresis system and 4–12% gradient pre-cast polyacrylamide gels under reducing conditions at 200 V for 45 min (Invitrogen). For KLK-SLPI reactions, protein mixtures were visualized by silver staining with the Silver Xpress kit (Invitrogen), according to the manufacturer's instructions. For KLK-LEKTI reactions, proteins were transferred to Hybond-C Extra nitrocellulose membrane (Amersham Biosciences) at 30 V for 1 h, blocked in Tris-buffered saline-Tween (TBS-T; 0.1 mol/liter Tris-HCl buffer (pH 7.5) containing 0.15 mol/liter NaCl and 0.1% Tween 20) supplemented with 5% nonfat dry milk overnight at 4 °C and probed with anti-LEKTI monoclonal antibody 1C11G6 (for rLEKTI(1–6), -(6–9′), and -(9–12)) or 1D6G8 (for rLEKTI(12–15)), both diluted 1:1,000 in TBS-T, for 1 h at room temperature. Membranes were washed three times for 15 min with Tris-buffered saline-Tween and treated with alkaline phosphatase-conjugated goat anti-mouse antibody (1:10,000 in Tris-buffered saline-Tween; Jackson ImmunoResearch Laboratories, West Grove, PA) for 1 h at room temperature. Finally, the membranes were washed again as above, and fluorescence was detected on x-ray film using a chemiluminescent substrate (Diagnostic Products Corp., Los Angeles, CA).

Effect of KLKs on SLPI Activity—Prior to measuring the inhibitory activity of SLPI against NE, individual KLKs were incubated with SLPI at several molar ratios (*i.e.* 1:5, 1:20, and 1:50) for different time points (0, 8, and 24 h) at 37 °C with gentle agitation. SLPI was also incubated alone for each time point, as a positive control. Samples from each time point were subsequent assayed for SLPI activity against NE, at NE to SLPI molar ratios of 1:1.25, 1:2.5, 1:5, and 1:10, using AAPV-AMC (0.1 mM) as a substrate. Free AMC fluorescence was measured on the Wallac 1420 Victor^{2TM} fluorometer for 20 min, as described above. NE-free reactions were used as negative controls, and background fluorescence was subtracted from each value. All experiments were performed in triplicate. (Note: the hydrolysis of AAPV-AMC by KLKs was not observed (data not shown).)

Pre-treatment and in Vitro Proteolysis of DSG1/Fc by KLKs—Prior to incubation with KLKs, DSG1/Fc (50 ng/μl, ~0.5 μM) was incubated at 37 °C with gentle agitation in the presence of either: 1) Tris-buffered saline (TBS; 20 mM Tris base, 140 mM NaCl, pH 7.6) for 1 h, 2) TBS containing 5 mM EGTA for 1 h, 3) TBS containing 1 mM $CaCl_2$ for 1 h, 4) TBS with 5 mM EGTA for 1 h, and then treated with TBS including 1 mM $CaCl_2$ for 1 h, 5) TBS with 1 mM $CaCl_2$ for 1 h, followed by the addition of 5 mM EGTA for 1 h. DSG1/Fc also was pre-treated as above in 0.1 M sodium acetate buffer (pH 5.4) in a total reaction volume of 70 μl. Proteolysis of DSG1/Fc was subsequently studied via incubation of individual KLKs (50 ng) with pre-treated DSG1/Fc (500 ng) in a final volume of 20 μl, in either TBS or sodium acetate, for various time intervals (0, 15 min, 30 min, 1 h, 2 h, 4 h, 8 h, and 24 h) at 37 °C with shaking. Reactions were stopped by freezing in liquid nitrogen. Proteins were separated by reducing SDS-PAGE and visualized by silver staining, as described above.

Effect of Calcium and EGTA on KLK Activity—KLK1, KLK5, KLK6, KLK13, and KLK14 (12 nM) were pre-treated with either: 1) TBS (pH 7.6), 2) sodium acetate buffer (pH 5.4), 3) TBS with 1 mM $CaCl_2$, 4) sodium acetate buffer with 1 mM $CaCl_2$, 5) TBS containing 1 mM $CaCl_2$ and 5 mM EGTA, and 6) sodium acetate buffer supplemented with 1 mM $CaCl_2$ and 5 mM EGTA, at a final volume of 100 μl in microtiter plate wells for 10 min at 37 °C with gentle agitation. Next, the appropriate AMC substrates for each KLK were applied to the wells at a final concentration of 0.5 mM. Free AMC fluorescence was measured on the Wallac 1420 Victor^{2TM} fluorometer for 20 min, as described above. KLK-free reactions were used as negative controls, and background fluorescence was subtracted from each value. All experiments were performed in triplicate.

N-terminal Sequencing—N-terminal sequence analysis was performed to identify KLK cleavage sites within SLPI and DSG1/Fc. KLKs (250 ng) were incubated with SLPI or DSG1/Fc (2.5 μg) for different time points as specified by the proteolysis experiments, separated by reducing SDS-PAGE, and transferred to a polyvinylidene difluoride membrane (Amersham Biosciences), previously immersed in 100% methanol, at 30 V for 1 h. After the transfer, the membrane was removed and rinsed with de-ionized water, stained with Coomassie Blue R-250 (0.1% solution in 40% methanol) for 5 min, and de-stained for 5 min in 50% methanol. The membrane was then thoroughly washed with de-ionized water and air-dried. SLPI and DSG1/Fc fragments were excised and subjected to automated N-terminal Edman degradation consisting of five cycles of Edman chemistry on a ABI 492 Procise cLC sequencer (Applied Biosystems, Foster City, CA), followed by analysis of resultant phenylthiohydantoin-amino acid residues on an high-performance liquid chromatography column.

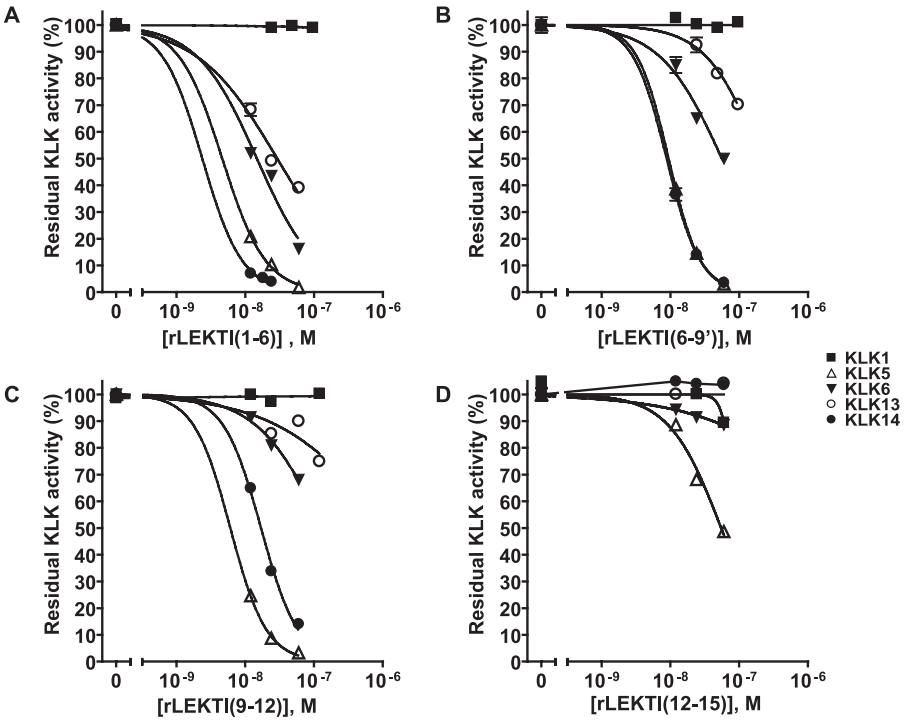

FIGURE 1. **Dose-dependent inhibition (IC_{50} determination) of KLK activity by rLEKTI fragments.** KLK1 (■), KLK5 (△), KLK6 (▼), KLK13 (○), and KLK14 (●) were incubated with increasing concentrations of rLEKTI(1–6) (*A*), rLEKTI(6–9′) (*B*), rLEKTI(9–12) (*C*), and rLEKTI(12–15) (*D*). Residual KLK activity was measured via proteolysis of AMC substrates (0.125–0.5 mM VPR-AMC for KLK5, KLK6, and KLK13; 0.125 mM QAR-AMC for KLK14) in the presence of rLEKTI divided by that of the uninhibited protease. Each data point represents mean ± S.E. of three independent assays. IC_{50} values are listed in Table 1.

TABLE 1
Inhibitory profile of rLEKTI fragments

LEKTI	KLK	IC_{50}	R^2	K_i	R^2
		nM		nM	
LEKTI(1–6)	KLK1	NI[a]			
	KLK5	4.62	0.9985	2.35 ± 0.22	0.995
	KLK6	14.73	0.9837	13.08 ± 2.36	0.975
	KLK13	29.10	0.9773	24.13 ± 3.82	0.984
	KLK14	2.368	0.9994	0.22 ± 0.021	0.998
LEKTI(6–9′)	KLK1	NI			
	KLK5	9.39	0.9987	4.68 ± 0.66	0.984
	KLK6	56.01	0.9566	47.58 ± 1.40	0.988
	KLK13	206.60	0.9300	222.12 ± 9.51	0.978
	KLK14	8.79	0.9970	3.41 ± 0.80	0.996
LEKTI(9–12)	KLK1	NI			
	KLK5	6.06	0.9986	2.75 ± 0.24	0.996
	KLK6	134.90	0.9671	195.32 ± 11.66	0.993
	KLK13	1172.00	0.7840	408.63 ± 16.47	0.988
	KLK14	16.95	0.9934	10.26 ± 1.25	0.984
LEKTI(12–15)	KLK1	NI			
	KLK5	54.68	0.9742	21.80 ± 2.40	0.990
	KLK6	NI			
	KLK13	NI			
	KLK14	NI			

[a] NI, no inhibition.

RESULTS

Multiple KLKs Are Inhibited by rLEKTI Fragments—Because KLKs represent likely physiological targets of LEKTI we tested rLEKTI fragments spanning all 15 domains for their inhibitory activity against the trypsin-like serine proteases KLK1, KLK5, KLK6, KLK13, and KLK14, *in vitro*.

Among the KLKs examined, KLK1 activity was uniquely unaffected after incubation with all rLEKTI fragments (Fig. 1), even in the presence of an 8- to 10-fold molar excess of rLEKTI or after different preincubation times (0–30 min). Furthermore, cleavage of rLEKTI fragments by KLK1 was not detected under the conditions used for kinetic inhibition assays (see Fig. 3). These results are in agreement with prior studies that demonstrate a lack of inhibition of the porcine ortholog of KLK1 by native and recombinant LEKTI domain 6 (37, 55).

The remaining KLKs were inhibited by rLEKTI fragments with IC_{50} and K_i values in the nanomolar range (Table 1 and Fig. 1) via non-competitive or mixed-type inhibitory mechanisms, as determined by Eadie-Hofstee plots (Fig. 2; *V versus V*/[*S*], where the slope is equal to $-K_m$ and the *y*-intercept is equal to V_{max}) and corresponding kinetic parameters (V_{max}, K_m; Tables 2–5). The overall rank order for KLK inhibition by rLEKTI fragments based on IC_{50} and K_i values from lowest to highest was: KLK5 ≈ KLK14 < KLK6 < KLK13, where values obtained for KLK5 and KLK14 values were consistently several orders of magnitude lower than those for KLK6 and KLK13 (Table 1). rLEKTI(1–6) was the most potent inhibitor for all KLKs tested (exclusive of KLK1), particularly for KLK5 and KLK14, with K_i values of 2.35 nM and 0.22 nM and IC_{50} values of 2.43 nM and 0.0051 nM, respectively. The concentration-dependent inhibition of KLKs by rLEKTI(1–6) is shown in Fig. 1*A*. As evident by the decrease in V_{max} and increase in K_m for KLK5, KLK6, KLK13, and KLK14 in the presence of increasing rLEKTI(1–6) concentrations, shown graphically via the Eadie-Hofstee plot (Fig. 2*A*), the inhibitory mechanisms were classified as mixed, *i.e.* containing both competitive and non-competitive components (Table 2).

rLEKTI(6–9′) and rLEKTI(9–12) also exerted strong mixed-type inhibitory activity against KLK5 and KLK14, with K_i values ranging from 2.75 to 10.26 nM (Tables 3 and 4 and Fig. 2*C*). These data are in general accordance with that of Schechter *et al.* (40), who recently published K_i values of 3.5–5.5 nM for the inhibition of KLK5 by rLEKTI(6–9′) and rLEKTI(9–12) at pH 8.0. In contrast to KLK5 and KLK14 inhibition, KLK6 and KLK13 activity was inhibited to a lower extent and in a non-competitive manner by rLEKTI(6–9′) and rLEKTI(9–12), as evidenced by the dose-response curves (Fig. 1, *B* and *C*) and the increase in V_{max} values accompanied by relatively constant K_m values in the presence of increasing rLEKTI(6–9′) and rLEKTI(9–12) concentrations (Tables 3 and 4 and Fig. 2*B*), respectively. Both KLK6 and KLK13 were also less effectively inhibited by rLEKTI(6–9′) and rLEKTI(9–12) than by rLEKTI(1–6) (Table 1). For example, the K_i values for the inhibition of KLK13 by rLEKTI(6–9′) and rLEKTI(9–12) were

10-fold and 20-fold higher, respectively, than for rLEKTI(1–6) inhibition. Interestingly, the KLK6 K_i values obtained for rLEKTI(6–9′) and rLEKTI(9–12) inhibition are comparable to those determined for KLK7, *i.e.* 11 nM and 220 nM, respectively (40).

KLK5 was the only KLK tested to be inhibited by rLEKTI(12–15) (Tables 1 and 5 and Figs. 1*D* and 3*D*), indicative of a stringent or unique specificity for this rLEKTI fragment. The observed lack of inhibitory activity of rLEKTI(12–15) against the other KLKs tested was unexpected based on the primary LEKTI sequence, which contains highly favorable P1-Arg active site residues within domains 12–14. Thus, the general inactivity of this fragment could be 1) attributed to the presence of a P1-Lys residue within domain 15, which is not highly preferred by KLK5, KLK6, KLK13, or KLK14 (45, 52–54) and is supported by the finding that rLEKTI domain 15 does not inhibit KLK5 (39) or 2) possibly due to an unfavorable tertiary structure (*e.g.* suboptimal backbone angles) within P3-P3′ regions, which form the canonical binding loops that interact with serine proteases. In the case of KLK14, the lack of detectable inhibition by rLEKTI(12–15) may be due to the rapid proteolysis and possible inactivation of this inhibitory fragment by KLK14 (Fig. 3*D*). We have recently identified a putative KLK14 cleavage site within LEKTI domain 15, *i.e.* $Arg^{1034} \downarrow Gln^{1035}$ (LEKTI numbering according to GenBank™ accession number NP_006837), by phage display substrate technology (47), which would give rise to a ~6.5-kDa fragment of rLEKTI(12–15).

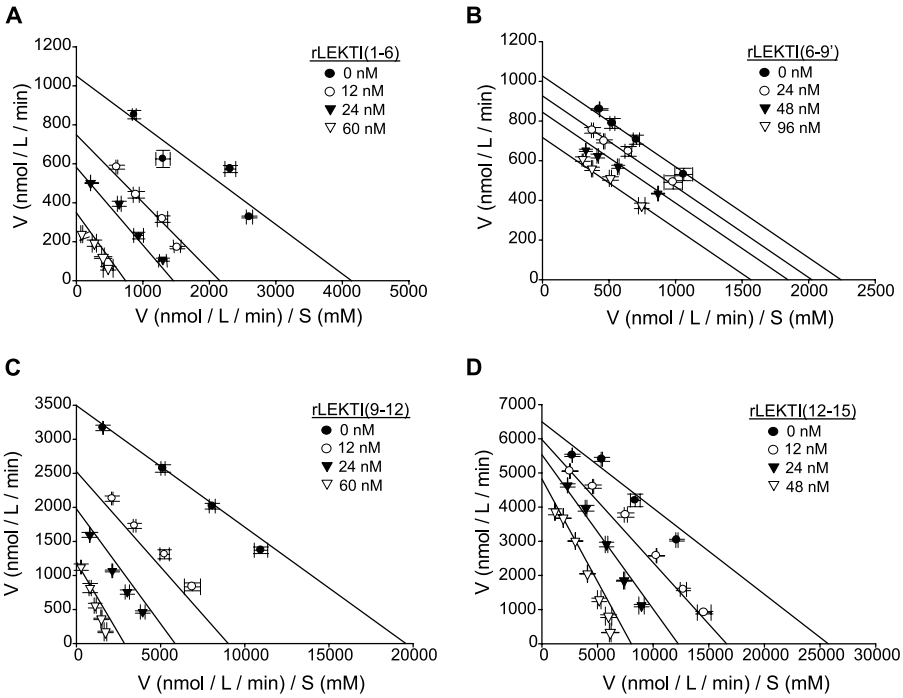

FIGURE 2. **Representative Eadie-Hofstee (*V versus V*/[*S*]) plots for the hydrolysis of AMC substrates by KLKs in the presence of rLEKTI fragments.** *A*, mixed-type inhibition of KLK6 by rLEKTI(1–6); *B*, non-competitive inhibition of KLK13 by rLEKTI(6–9′); *C*, mixed-type inhibition of KLK14 by rLEKTI(9–12); and *D*, mixed-type inhibition of KLK5 by rLEKTI(12–15). Each data point corresponds to mean values ± S.E. of triplicate measures of a representative experiment. The *solid lines* represent the linear regression fits.

Due to its classification as a reversible, tight-binding, "standard" mechanism inhibitor, LEKTI acts as highly specific protease substrate, which mediates inhibition through cleavage of a reactive site bond by the cognate protease (56, 57). Typically, hydrolysis of the inhibitor is extremely slow and does not proceed to completion (57). Thus, the stability of rLEKTI fragments against KLK proteolysis and of KLK/rLEKTI complexes was also investigated (Fig. 3). Relative rates of proteolysis were determined upon examination of the decrease in intensity of intact rLEKTI bands over time. rLEKTI fragments were generally resistant to digestion by KLKs, with the exception of the complete hydrolysis of: rLEKTI(6–9′) by KLK6 after 24 h (Fig. 3*B*), rLEKTI(9–12) by KLK6 and KLK14 after 4 h (Fig. 3*C*) and rLEKTI(12–15) by KLK14 after 1 h (Fig. 3*D*).

TABLE 2
Classification of rLEKTI(1–6) inhibitory mechanisms

KLK	rLEKTI(1–6)	V_{max}	K_m	R^2	Inhibitory mechanism
	nM	nmol liter^{-1} min^{-1}	mM		
KLK1	NI[a]				
KLK5	0	2884 ± 35	0.46 ± 0.019	0.997	Mixed
	12	1140 ± 18	0.93 ± 0.040	0.997	
	24	1028 ± 44	1.88 ± 0.16	0.993	
	60	350 ± 15	3.72 ± 0.26	0.998	
KLK6	0	912 ± 9	0.23 ± 0.012	0.996	Mixed
	12	653 ± 11	0.29 ± 0.019	0.987	
	24	580 ± 9	0.33 ± 0.020	0.990	
	60	266 ± 6	0.43 ± 0.030	0.989	
KLK13	0	777 ± 12	0.48 ± 0.025	0.995	Mixed
	12	712 ± 10	0.57 ± 0.025	0.996	
	24	534 ± 7	0.64 ± 0.025	0.997	
	60	506 ± 8	0.82 ± 0.035	0.997	
KLK14	0	6965 ± 127	0.12 ± 0.0073	0.986	Mixed
	12	1428 ± 84	1.34 ± 0.15	0.990	
	18	1195 ± 35	1.45 ± 0.091	0.996	
	24	962 ± 9	1.53 ± 0.032	1.000	

[a] NI, no inhibition.

TABLE 3
Classification of rLEKTI(6–9′) inhibitory mechanisms

KLK	rLEKTI(6–9′)	V_{max}	K_m	R^2	Inhibitory mechanism
	nM	nmol liter^{-1} min^{-1}	mM		
KLK1	NI[a]				
KLK5	0	2829 ± 34	0.44 ± 0.021	0.996	Mixed
	12	1640 ± 20	0.67 ± 0.027	0.997	
	24	1079 ± 24	1.41 ± 0.072	0.997	
	60	451 ± 21	2.96 ± 0.024	0.997	
KLK6	0	1186 ± 15	0.44 ± 0.021	0.989	Non-competitive
	12	958 ± 14	0.36 ± 0.021	0.984	
	24	709 ± 13	0.32 ± 0.025	0.980	
	60	501 ± 4	0.32 ± 0.012	0.996	
KLK13	0	1069 ± 24	0.51 ± 0.038	0.981	Non-competitive
	12	905 ± 20	0.42 ± 0.034	0.974	
	24	788 ± 8	0.40 ± 0.015	0.995	
	60	757 ± 12	0.51 ± 0.027	0.991	
KLK14	0	4186 ± 123	0.25 ± 0.021	0.984	Mixed
	24	739 ± 17	0.32 ± 0.027	0.985	
	60	171 ± 3	0.33 ± 0.018	0.994	

[a] NI, no inhibition.

TABLE 4
Classification of rLEKTI(9–12) inhibitory mechanisms

KLK	rLEKTI(9–12)	V_{max}	K_m	R^2	Inhibitory mechanism
	nM	nmol liter^{-1} min^{-1}	mM		
KLK1	NI[a]				
KLK5	0	2795 ± 33	0.44 ± 0.019	0.997	Mixed
	12	1144 ± 26	0.75 ± 0.049	0.992	
	24	823 ± 24	1.66 ± 0.011	0.997	
	60	707 ± 62	5.09 ± 0.064	0.996	
KLK6	0	937 ± 16	0.14 ± 0.0077	0.991	Non-competitive
	12	893 ± 17	0.28 ± 0.020	0.985	
	24	698 ± 11	0.24 ± 0.018	0.984	
	60	593 ± 8	0.25 ± 0.018	0.986	
KLK13	0	1064 ± 19	0.50 ± 0.030	0.988	Non-competitive
	60	868 ± 11	0.40 ± 0.021	0.993	
	120	832 ± 17	0.52 ± 0.034	0.986	
KLK14	0	3480 ± 34	0.18 ± 0.0061	0.996	Mixed
	12	2608 ± 61	0.23 ± 0.016	0.989	
	24	1901 ± 20	0.38 ± 0.011	0.998	
	60	1326 ± 29	0.68 ± 0.041	0.992	

[a] NI, no inhibition.

TABLE 5
Classification of rLEKTI(12–15) inhibitory mechanisms

KLK	rLEKTI(12–15)	V_{max}	K_m	R^2	Inhibitory mechanism
	nM	nmol liter^{-1} min^{-1}	mM		
KLK1	NI[a]				
KLK5	0	6279 ± 113	0.27 ± 0.015	0.995	Mixed
	12	5991 ± 77	0.32 ± 0.012	0.996	
	24	5598 ± 92	0.47 ± 0.024	0.994	
	60	4796 ± 66	0.65 ± 0.026	0.997	
KLK6	NI				
KLK13	NI				
KLK14	NI				

[a] NI, no inhibition.

rLEKTI(1–6) and rLEKTI(6–9′) were digested at a slower rate by KLK5 (Fig. 3, *A* and *B*) as was rLEKTI(12–15) by KLK13 (Fig. 3*D*). Notably, rLEKTI(1–6) was not fully degraded by any KLK, suggesting that it may have a longer half-life than other rLEKTI fragments (data not shown), which may be due to a unique domain conformation. With respect to the KLKs that were inhibited by rLEKTI fragments, most did not recover their activities even after 24 h, except for the few examples described above. Taken together, rLEKTI fragments exhibited both permanent (pseudoirreversible) and temporary (reversible) behavior, depending on the KLK/LEKTI fragment combination. Temporary inhibition of trypsin by native and recombinant LEKTI domain 6 was also observed, as evidenced by trypsin digestion of the inhibitor at the reactive site after a 1-h incubation, indicative of a short-lived, unstable trypsin-LEKTI complex (55). This instability was attributed to the presence of only two of three disulfide bridges that characterize Kazal-type inhibitors within the LEKTI domain 6 (55). Furthermore, our results suggest that rLEKTI fragments function as intact, multidomain fragments and need not be processed into single domains to be active, as previously postulated (31).

KLK Activity Is Not Inhibited by SLPI or Elafin—SLPI (58) and elafin/SKALP (59) are present in the stratum corneum and are implicated in desquamation. For instance, both SLPI and elafin can inhibit corneocyte shedding *in vitro* and inhibit KLK7 activity (41), some NS patients do not display increased epider-

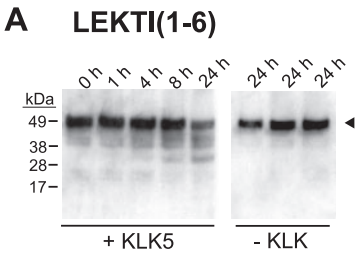

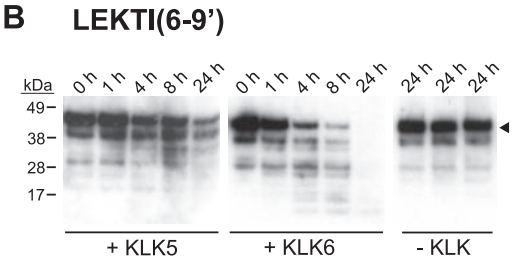

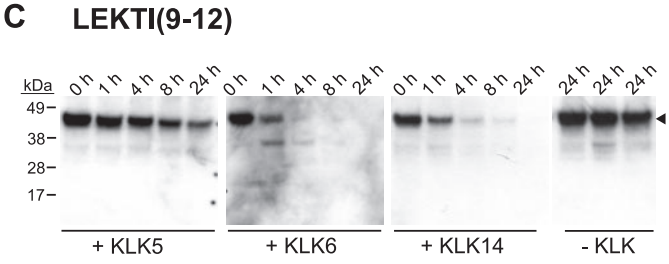

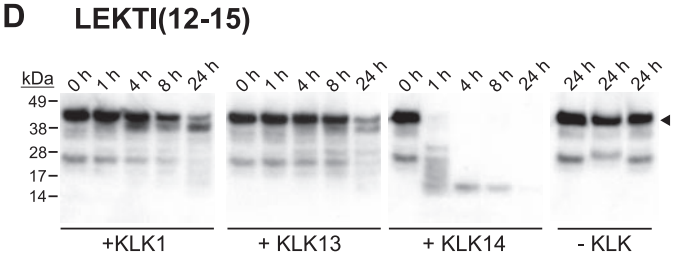

FIGURE 3. **Immunodetection of rLEKTI(1–6) (*A*), rLEKTI(6–9′) (*B*), rLEKTI(9–12) (*C*), and rLEKTI(12–15) (*D*) after incubation with individual KLKs.** rLEKTI fragments (10 ng) were incubated with individual KLKs (1 ng) in optimal KLK reaction buffer for various time points (0, 1, 4, 8, and 24 h) at 37 °C. Reactions were terminated and separated by SDS-PAGE followed by Western blotting using anti-LEKTI monoclonal antibody 1C11G6 (1:1000; for rLEKTI domains 1–6, 6–9′, and 9–12) or 1D6G8 (1:1000; for rLEKTI domains 12–15). rLEKTI fragments were incubated alone for 24 h in each optimal KLK reaction buffer (−*KLK lanes*). The *solid arrowhead* (▲) indicates intact rLEKTI fragments. Molecular mass standards (kilodaltons) are indicated on the *left*.

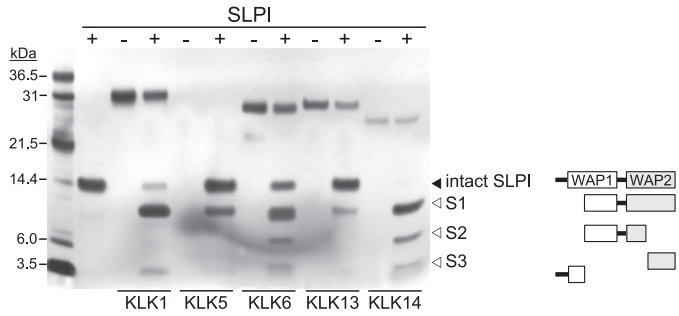

FIGURE 4. **SDS-PAGE analysis of SLPI after incubation with KLKs.** SLPI (500 ng) was incubated with KLK1, KLK5, KLK6, KLK13, and KLK14 (50 ng) for 24 h at 37 °C. SLPI (*SLPI+ lane*) and individual KLKs (*SLPI− lanes*) were also incubated alone. Reactions were terminated and separated by SDS-PAGE followed by silver staining. The *solid arrowhead* indicates intact SLPI and *open arrowheads* indicate KLK-generated SLPI fragments. SLPI fragments subjected to N-terminal sequence analysis are labeled "*S1–S7*" on the *right*, and the results are listed in Table 6. A schematic representation of KLK-mediated SLPI cleavage is shown on the *right*. Molecular mass standards (kilodaltons) are indicated on the *left*.

mal serine protease activity, indicating that other SPI are present to attenuate serine protease function (25), and elafin is overexpressed in the epidermis of NS patients (50, 60). This prompted us to test the hypothesis that additional KLKs may be targeted by these two inhibitors. However, unlike the effect of elafin and SLPI on KLK7, no demonstrable inhibitory activity was found against any KLK studied under the experimental conditions chosen, even at a 100-fold molar excess of either inhibitor (data not shown). These results are likely explained by the presence of P1-Leu^{72} and P1-Ala^{84} within the reactive sites of SLPI (61) and elafin (62), respectively, both of which are unfavorable P1 amino acids for the KLKs tested. (Note: the numbering starts from the mature SLPI sequence and the elafin preproprotein sequence according to GenBank^{TM} accession numbers NP_003055 and NP_002629, respectively). Similarly, lack of inhibition of KLK3 (also known as prostate-specific antigen) by SLPI has also been reported (63).

Proteolytic Processing of SLPI by KLKs—The incubation of SLPI with individual KLKs at a 26:1 molar ratio for 24 h resulted in the generation of 2 or 4 SLPI degradation products, depending on the KLK (Fig. 4). Intact SLPI was visualized as a ~12-kDa band and contains two C-terminal whey acidic protein (WAP) domains, whereby the first possesses antimicrobial activity (64) and the second harbors inhibitory activity (65). KLK14 was able to completely degrade intact SLPI after 24 h; lower hydrolysis rates were exhibited by KLK1, followed by KLK6, KLK5, and KLK13. Due to cleavage at peptide bond Arg^{20}–Tyr^{21} within the first WAP domain, all KLKs produced two SLPI fragments of 9.6 kDa (S1; Tyr^{21}–Ala^{132}) and 2 kDa (Ser^{1}–Arg^{20}) (Table 6). An additional cleavage site was identified for KLK6 and KLK14 within the second WAP domain at Leu^{72}–Met^{73}, which generated another two SLPI fragments of 5.8 kDa (S2; Tyr^{21}–Leu^{72}) and 3.5 kDa (S3; Met^{73}–Ala^{132}). Although P1-Leu is not a preferred amino acid for either KLK, the observed cleavage may be due to the relative exposure and susceptibility of the reactive site Leu^{72}–Met^{73} bond to protease attack and/or the importance of other residues, in addition to P1, to protease specificity.

The presence of KLK6 and KLK14 cleavage sites within the second WAP domain of SLPI, which contains the reactive site P1-Leu^{72} for protease inhibition, impelled us to examine whether KLKs could inactivate SLPI and thereby diminish its inhibitory activity against NE. Upon incubation with both KLK6 and KLK14, SLPI activity was decreased to only 90% of control (*i.e.* SLPI alone). However, this may not be significant compared with cathepsins L and S, which have been shown to completely abrogate SLPI activity against NE in a 1-h time period (66). The reason(s) for this disparity are not clear, but may be attributed to the location and number of the cathepsin and KLK cleavage sites within the second WAP domain. Cathepsins cleave SLPI at two sites, *i.e.* Thr^{68}–Tyr^{69} and Met^{73}–Leu^{74}, and may affect the structure of the intervening region, Tyr^{69}–Met^{73}, which is involved in binding SLPI target proteases (66, 67). In contrast, KLK6 and KLK14 cleave solely after

TABLE 6
N-terminal sequence analysis of KLK-generated SLPI and DSG1/Fc fragments and putative KLK cleavage sites

Fragment	N-terminal sequence[a]	KLK	KLK cleavage site location within intact molecule
SLPI			
S1/2	(Arg^{20}) ↓ YKKPE[b]	KLK1, KLK6, and KLK14	First WAP[c] domain
S3	(Leu^{72}) ↓ MLNPPN	KLK6 and KLK14	Second WAP domain
DSG1/Fc			
1A	(Lys^{197}) ↓ IIRQEP[d]	KLK1	Second CAD[e] domain
1B	(Lys^{445}) ↓ NKVTKE		Fourth CAD domain
5A/D	(Arg^{242}) ↓ DGGADG	KLK5	Second CAD domain
5B	(Arg^{422}) ↓ YVMGNN		Fourth CAD domain
5C	(Arg^{146}) ↓ VLDIND		First CAD domain (Ca^{2+} binding motif)
6A	(Lys^{368}) ↓ ASKIX[f]X	KLK6	Third CAD domain (Ca^{2+} binding motif)
6B	(Arg^{422}) ↓ YVMGNN		Fourth CAD domain
14A/B	(Tyr^{528}) ↓ SSEPGN	KLK14	Between fourth CAD domain and TM[g] region

[a] The N-terminal sequence is preceded by the putative KLK cleavage site (↓) with the P1 amino acid in parentheses.
[b] Numbering starts from the mature SLPI sequence (GenBank™ accession number NP_003055).
[c] WAP, whey acidic protein domain (also known as the four-disulfide core domain).
[d] Numbering starts from desmoglein 1 preproprotein sequence (GenBank™ accession number NP_001933).
[e] CAD, cadherin repeat domain.
[f] The amino acid was not determined.
[g] TM, transmembrane region.

the active site P1-Leu^{72} and do not disrupt the protease binding site or significantly alter the structure of SLPI. Further stabilization of KLK6- and KLK14-cleaved SLPI conformation is likely provided by the four disulfide bridges within the WAP domain, which thereby facilitates SLPI inhibition of NE, even in the presence of these two KLKs. Moreover, cleavage at P1-R^{20} by all KLKs tested could possibly abrogate the antibacterial activity of SLPI. The consequences of KLK-mediated digestion of SLPI are to be determined.

KLK-mediated Proteolysis of DSG1—A prerequisite for stratum corneum desquamation is the degradation of the desmosomal cadherin, DSG1 (8, 9). KLKs are implicated in DSG1 proteolysis due to: 1) their colocalization with DSG1 in the stratum corneum, 2) the *in vitro* digestion of DSG1 within epidermal extracts by KLK5 (24), and 3) the correlation between decreased DSG1 levels and elevated KLK activity within the epidermis of NS patients (25). Given this, we examined whether DSG1 could serve as a substrate for KLK1, KLK6, KLK13, and KLK14, in addition to KLK5, *in vitro*. DSG1/Fc, a chimeric protein formed of the five extracellular domains of DSG1 followed by a peptide linker and the Fc region of human IgG_1, was incubated with KLKs for increasing time periods at pH 5.4, within the acidic pH range of the stratum corneum (68), and at pH 7.6, within the optimal pH range for KLK activity (Fig. 5). In all cases, no degradation of DSG1/Fc was observed in the absence of KLKs (Fig. 5, *A–D*, *lane 2*). Relative KLK cleavage efficiencies were assessed by the decrease in intact DSG1/Fc band intensity over time. As expected, higher KLK activity was generally observed at pH 7.6 rather than pH 5.4, and despite their similar specificity for P1-Arg, each KLK produced a distinct DSG1/Fc cleavage pattern and cleaved at unique sites (Fig. 5 and Table 6). No detectable digestion of DSG1/Fc by KLK13 was found at either pH tested, even after 24 h of incubation (data not shown). KLK1 showed minimal activity against DSG1/Fc at pH 5.4, which was slightly elevated at pH 7.6, allowing for the determination of two putative cleavage sites at K^{197}–Ile^{198} and K^{445}–Asn^{446} (Table 6).

The remaining KLKs demonstrated comparably higher DSG1/Fc cleavage rates, with a rank order of KLK6 < KLK5 ≪ KLK14, from lowest to highest efficiency. As indicated in Fig. 5*C*, KLK6 generated three major DSG1/Fc fragments of ~66, 55, and 50 kDa, the latter two of which were denoted 6A and 6B and resulted from the cleavage at Lys^{368}–Ala^{369} and R^{422}–Tyr^{423} (Table 6). In contrast, KLK5 induced a relatively faster decrease in intact DSG1/Fc and generated a multitude of DSG1/Fc degradation products. The N-terminal sequence of four major DSG1/Fc fragments of ~66, 45, 36, and 25 kDa (Fig. 5, *A–D*, respectively) was identified, and permitted us to determine three putative cleavage sites at Arg^{146}–Val^{147}, Arg^{242}–Asp^{243}, and Arg^{422}–Tyr^{423} (Table 6). These results agree with those of Caubet *et al.* (24), who demonstrated efficient KLK5-mediated degradation of DSG1 within epidermal extracts at pH 5.4. Undoubtedly, DSG1/Fc was the best substrate for KLK14. Complete digestion of intact DSG1/Fc was demonstrated in the presence of KLK14 after 30 min at pH 5.4 and 5 min at pH 7.6 (Fig. 5*D*). Two major cleavage products of ~40 and 37 kDa (14A and 14B, respectively) were obtained, and were not further degraded after a 24-h incubation period (data not shown). The N terminus of both 14A and 14B fragments was Ser^{529}-Ser-Glu-Pro-Gly-Asn, suggestive of cleavage at the Tyr^{528}–Ser^{529} peptide bond. The P1-Tyr specificity of KLK14 is not surprising as we previously determined that KLK14 is a dual specificity enzyme with both trypsin and chymotrypsin-like activity (47).

Given that calcium is essential for the stabilized conformation and adhesive function of cadherins such as DSG1 (4) we addressed whether the presence/absence of calcium would affect the susceptibility of DSG1 to proteolysis by KLKs. To this end, DSG1/Fc was pre-treated with 1 mM $CaCl_2$ and/or 5 mM EGTA, a chelator with high selectivity for Ca^{2+} ions in two buffer systems, TBS (pH 7.6) and sodium acetate (pH 5.4). As a control, DSG1/Fc was also pre-treated in buffer only, *i.e.* in the absence of $CaCl_2$ and EGTA, as in the time-course experiments. A significant effect on KLK activity by $CaCl_2$ and EGTA was not observed (data not shown). As shown in Fig. 6, the presence of either EGTA or $CaCl_2$ did not influence the efficiency of DSG1/Fc digestion by KLKs, under the experimental conditions chosen. Hence, the calcium-stabilized conformation of DSG1 may not be required for KLK-mediated cleavage. This is also the case for other serine proteases such as trypsin and V8 proteinase, but not for exfoliative toxins, which can only cleave

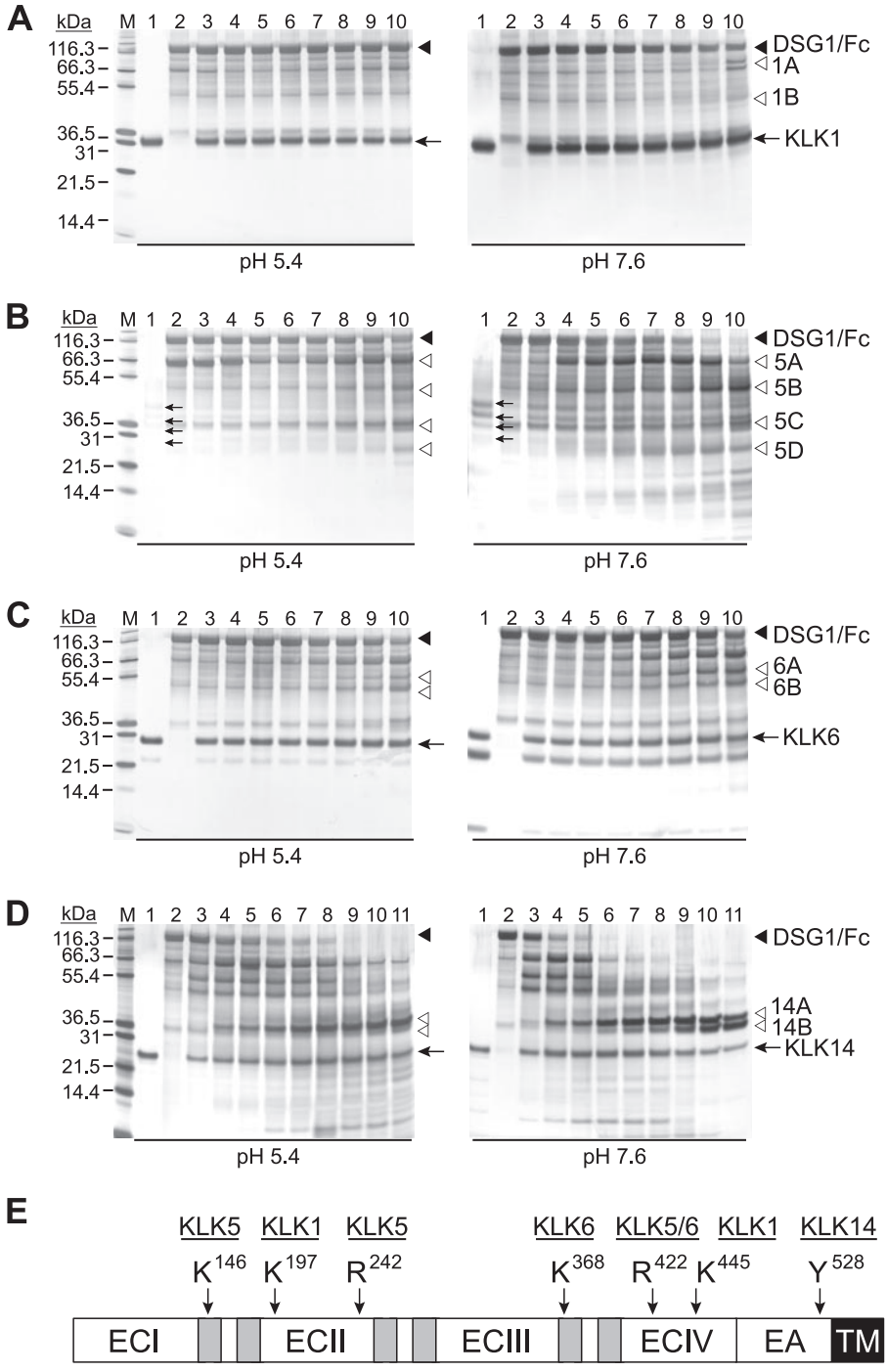

FIGURE 5. **Time-dependent digestion of DSG1/Fc by KLKs and putative KLK cleavage sites.** DSG1/Fc (500 ng) was incubated with 50 ng of KLK1 (*A*), KLK5 (*B*), KLK6 (*C*), and KLK14 (*D*) for increasing time periods at 37 °C. Reactions were carried out at both pH 5.4 and pH 7.6, as indicated below gel images, terminated, resolved by reducing SDS-PAGE, and visualized by silver staining. *Lane 1*, KLKs incubated alone for 24 h (*A–C*) and 2 h (*D*). *Lane 2*, DSG1/Fc incubated alone for 24 h (*A–D*) and 2 h (*E*). For *A–C*, *lanes 3–10* represent 0, 0.25, 0.5, 1, 2, 4, 8, and 24 h time points, respectively. For *D*, *lanes 3–11* indicate 0, 1, 2, 5, 10, 15, 30, 60, and 120 min time points, respectively. *Solid arrowheads* indicate intact DSG1/Fc; *open arrowheads* and labels (*i.e. 1A*, *1B*, etc.) denote KLK-generated DSG1/Fc fragments subjected to N-terminal sequence analysis (results are listed in Table 6). *Arrows* indicate KLK protein bands (KLK5, shown in *lane* of *B*, is represented by four protein bands). *M*, molecular mass standards in kilodaltons. *E*, location of KLK cleavage sites within the extracellular domains of DSG1. *Downward arrows* denote the location of KLK cleavage sites (P1 amino acid is shown; numbering starts from desmoglein 1 preproprotein sequence (GenBank™ accession number NP_001933)). *Gray boxes* denote the calcium binding motifs. *ECI-ECIV*, extracellular cadherin repeat domains I–IV; *EA*, extracellular anchor; *TM*, transmembrane region.

DSG1 in the presence of calcium (69), exclusively within a calcium binding site at Glu^{381}–Gly^{382} (70).

DISCUSSION

Stratum corneum desquamation is a tightly regulated process, orchestrated by the concerted function of serine proteases and SPI within the intercorneal matrix. To date, serine protease action in the stratum corneum has been linked to two members of the human kallikrein family: KLK5 and KLK7. Yet, besides KLK5 and KLK7, it is now recognized that an additional nine KLKs are expressed in the uppermost epidermal layers (26). Among these, the stratum corneum levels of six KLKs have been quantified (29), and one, namely KLK14, has been recently purified from the stratum corneum in its active form (30). The present study is the first to support a role for kallikreins other than KLK5 and KLK7, namely KLK6, KLK13, and KLK14, as desquamatory enzymes, as indicated by their efficient digestion of DSG1 and/or their potent inhibition by LEKTI, *in vitro*.

Unregulated desquamation drives and sustains the phenotype of NS, an inherited skin disorder in which the serine protease/SPI balance is tipped in favor of serine proteases, due to mutations in the gene encoding LEKTI. This study is the first to profile the inhibitory capacity of all 15 inhibitory LEKTI domains against multiple KLKs, summarized in Fig. 7. Our *in vitro* data indicate that KLK5, KLK6, KLK13, and KLK14 are significantly inhibited by rLEKTI fragments. To establish the *in vivo* significance of protease-inhibitor interactions, the determination of *in vitro* kinetic parameters (*e.g.* K_i) as well as the *in vivo* inhibitor concentration are generally required (71, 72). Although *in vivo* LEKTI stratum corneum concentrations are currently unknown, in the case of KLK-LEKTI interactions, the resultant low K_i constants (in the nanomolar range), which indicate the formation of relatively stable KLK-LEKTI complexes and

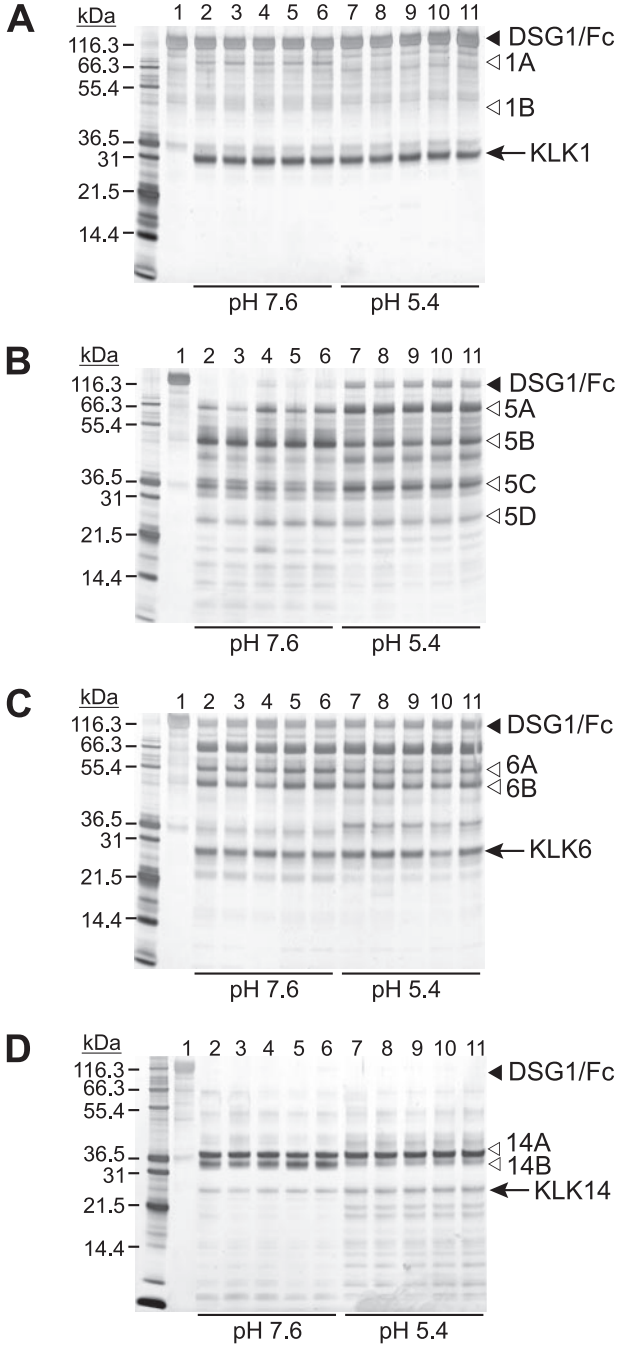

FIGURE 6. **SDS-PAGE analysis of pre-treated DSG1/Fc after incubation with KLKs.** DSG1/Fc (500 ng) was incubated with 50 ng of KLK1 (*A*), KLK5 (*B*), KLK6 for 24 h (*C*), and KLK14 (*D*) for 2 h at 37 °C. *Lane 1*, DSG1/Fc incubated alone for 24 h (*A–C*) and 2 h (*D*), negative control. *Lanes 2–6*, reactions performed in TBS at pH 7.6; *lanes 7–11*, reactions carried out in sodium acetate buffer at pH 5.4. DSG1/Fc was pre-treated under various conditions prior to incubation with KLKs. *Lanes 2* and *7*, DSG1/Fc pre-treated in buffer only; *lanes 3* and *8*, DSG1/Fc pre-treated in buffer containing 5 mM EGTA; *lanes 4* and *9*, DSG1/Fc pre-treated in buffer with 1 mM $CaCl_2$; *lanes 5* and *10*, DSG1/Fc pre-treated in buffer with 5 mM EGTA, followed by the addition of 1 mM $CaCl_2$; *lanes 6* and *11*, DSG1/Fc pre-treated in buffer containing 1 mM $CaCl_2$ followed by the addition of 5 mM EGTA. Reactions were terminated and separated by SDS-PAGE followed by silver staining. *Solid arrowheads* indicate intact DSG1/Fc; *open arrowheads* and corresponding labels (*i.e. 1A*, *1B*, etc.) denote KLK-generated DSG1/Fc fragments subjected to N-terminal sequence analysis (results are listed in Table 6). *Arrows* indicate KLK protein bands. Molecular mass standards (kilodaltons) are shown on the *left*. Note that the protein band corresponding to KLK5 is masked by KLK5-generated DSG1/Fc fragments.

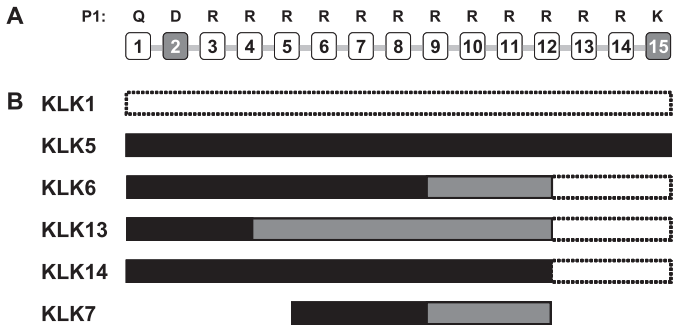

FIGURE 7. **Summary of rLEKTI inhibition of KLKs.** *A*, organization of LEKTI inhibitory domains (GenBank™ accession number NP_006837). *Gray boxes* denote Kazal-type inhibitory domains (three disulfide bonds); *white boxes* represent non-Kazal-type domains (two disulfide bonds). The identity of the active site P1 residue is indicated above each domain. *B*, *boxes* indicate strength of LEKTI inhibition of individual KLKs based on K_i values. *White boxes* indicate no inhibition; *gray boxes* indicate moderate inhibition ($K_i > 200$ nM); *black boxes* represent strong inhibition ($K_i < 50$ nM). KLK7 data are derived from the study by Schechter *et al.* (40). Not shown is the lack of inhibition of domain 6 toward KLK1 (37, 55) and of domain 15 against KLK5 and KLK7 (39).

strong inhibition, along with the *in vivo* colocalization of KLKs and LEKTI in the stratum granulosum and stratum corneum and the KLK/LEKTI imbalance observed in NS, strongly suggest that KLKs are physiological targets of LEKTI.

Notably, the individual rLEKTI fragments utilized in the present study and by Schechter *et al.* (40) display distinct inhibitory specificities against the KLKs examined thus far (Fig. 7). Generally, LEKTI domains 1–8 can potently inhibit multiple KLKs; yet domains 9–12 exhibit a higher specificity toward KLK5 and KLK14, whereas domains 12–15 can only inhibit KLK5. This suggests that each domain or fragment may have one or more preferred protease targets *in vivo*. Although these rLEKTI fragments may not be fully representative of physiological LEKTI forms, accumulating studies suggest that post-translational processing of LEKTI occurs *in vitro* and *in vivo*. For instance, LEKTI domains 1, 5, and 6 have been isolated from human blood filtrates (37, 73), and several multidomain LEKTI fragments ranging from 30 to 68 kDa are present in the conditioned media of normal primary human keratinocytes (38, 48, 74, 75), indicating that both single and multidomain fragments of LEKTI occur naturally.

Inhibition of KLK activity by rLEKTI fragments occurred via non-competitive or mixed-type mechanisms. Jayakumar *et al.* (49) previously proposed that the non-competitive inhibitory action of rLEKTI(6–9′) could be due to the interaction between 1) the canonical loop of one inhibitory domain with the catalytic site of the protease and 2) the binding of a second inhibitory domain to an allosteric site within the protease. Similar reasons could account for the observed inhibitory mechanisms of rLEKTI on KLKs. Further studies are warranted to clarify these findings.

SLPI and elafin/SKALP are implicated in the regulation of desquamation, yet neither inhibitor could attenuate the activity of any KLK studied. Putative targets of SLPI and elafin inhibitory action within the skin may include KLK7 (41) and elastase I, which is expressed by cultured primary keratinocytes (76) and is known to interact with these inhibitors in other tissues, *in vivo*. Moreover, KLK1 activity was not attenuated by any of the SPIs studied. These results were particularly unexpected for

LEKTI, which harbors P1-Arg in the majority of its inhibitory domains, a residue that is highly favored by KLK1 (51). However, KLK1 possesses a strong preference for large hydrophobic residues at P2 (77, 78) and for basic residues at P3 (79). Thus, the presence of P2-Thr/Pro and P3-Cys within LEKTI inhibitory domains may explain, in part, the resistance of KLK1 to inhibition by LEKTI. The regulation of KLK activity, particularly KLK1, by other SPIs in the epidermis, *i.e.* α_2-macroglobulin-like-1 (42), protein C inhibitor (80), and plasminogen activator inhibitor-2 (81), may be worth examining in the future.

As a (corneo)desmosomal adhesion molecule, DSG1 is essential for the maintenance of epidermal integrity (4), as evidenced by various inherited and acquired skin diseases that target DSG1 (82). Previous studies have shown that KLK5 can digest DSG1 *in vitro* (24) and that an association between premature DSG1 degradation and elevated KLK activity in the epidermis of NS patients exists (25). In the work presented here, we provide evidence for the direct cleavage of DSG1 by KLK1, KLK5, KLK6, and KLK14 and identify a number of putative cleavage sites, *in vitro*. Four KLK cleavage sites occur within the first three extracellular cadherin repeat domains (EC1–ECIII), which mediate heterophilic binding to desmocollins (*e.g.* desmocollin-1) (83). Among these sites, two reside within calcium binding motifs, responsible for the calcium-dependent conformation needed for proper DSG1 function. Interestingly, the KLK14 cleavage site is located a few amino acids N-terminal to the transmembrane domain, which would result in shedding of the entire ectodomain of DSG1. Thus, based on the location of KLK cleavage sites, the coordinated action of several KLKs might destabilize DSG1 structure and abolish adhesion to desmocollins on neighboring corneocytes. Moreover, extracellular DSG1 proteolytic fragments generated by KLKs may further perturb intercellular adhesion by competing with intact DSG1 and desmocollin-1 molecules for binding, as shown for soluble E-cadherin ectodomain fragments (84). Ultimately, KLK action could lead to corneocyte dyshesion during normal epidermal turnover but can result in overdesquamation and an impairment of epidermal barrier function when it is unopposed as in NS (25, 31–33).

Given the above, the results of our study may have important therapeutic implications for the treatment of skin disorders characterized by dysregulated KLK activity. We and others (39, 40) have shown that LEKTI has a potent inhibitory capacity for several KLKs. Hence, the administration of LEKTI as a therapeutic agent, to balance its deficiency in NS and/or of other KLK-specific inhibitors, to attenuate unopposed KLK activity observed in other diseases, could result in the restoration of epidermal integrity, permeability barrier function and a reduction of pro-inflammatory responses.

It has been postulated that the clinical severity of NS is correlated with the location of mutations within the *SPINK5* gene (31). That is, NS patients with mutations near the 3′-end of *SPINK5* encode LEKTI forms with a higher number of inhibitory domains than those whose mutation reside near the 5′-end. Accordingly, the degree of serine protease/SPI imbalance in the former will be lower than in the latter, resulting in a moderate increase in serine protease activity and hence, a less severe disease phenotype (31). As aforementioned, rLEKTI fragments display distinct inhibitory profiles against KLKs (Fig. 7). Hence, the lack of specific LEKTI domains in NS may lead to the elevation in the activity of only certain KLKs (*e.g.* deficiency of domains 12–15 may cause an increase in KLK5 activity specifically). Taken together, our data could allow for the development of tailored therapeutic strategies for subgroups of NS patients with distinct *SPINK5* mutations and corresponding clinical severities. For instance, NS patients with downstream mutations may benefit from the administration of LEKTI(12–15) or another inhibitor that targets KLK5 specifically, whereas patients with upstream mutations may require the suppression of multiple KLKs via LEKTI(1–6) or a more general SPI.

In conclusion, our results clearly demonstrate that multiple KLKs are potently inhibited by LEKTI and are able to efficiently degrade DSG1, *in vitro*. This study further substantiates the role of KLK5 as a desquamatory protease and also reveals that KLK6, KLK13, and particularly KLK14 may contribute to epidermal turnover and homeostasis under normal and pathological conditions. Accordingly, the suppression of KLK activity by LEKTI and/or other specific inhibitors may represent novel therapeutic strategies for the treatment of various skin diseases.

Acknowledgments—We thank Drs. Michael Blaber and Sachiko I. Blaber (Florida State University), and Isobel A. Scarisbrick (Mayo Medical and Graduate School, Rochester, MN) for providing purified recombinant human kallikreins 1 and 6.

REFERENCES

1. Brody, I. (1968) *Acta Derm. Venereol.* **48,** 290–302
2. Skerrow, C. J., Clelland, D. G., and Skerrow, D. (1989) *J. Cell Sci.* **92,** 667–677
3. Serre, G., Mils, V., Haftek, M., Vincent, C., Croute, F., Reano, A., Ouhayoun, J. P., Bettinger, S., and Soleilhavoup, J. P. (1991) *J. Invest. Dermatol.* **97,** 1061–1072
4. Green, K. J., and Gaudry, C. A. (2000) *Nat. Rev. Mol. Cell Biol.* **1,** 208–216
5. Kurzen, H., Moll, I., Moll, R., Schafer, S., Simics, E., Amagai, M., Wheelock, M. J., and Franke, W. W. (1998) *Differentiation* **63,** 295–304
6. Koch, P. J., Goldschmidt, M. D., Zimbelmann, R., Troyanovsky, R., and Franke, W. W. (1992) *Proc. Natl. Acad. Sci. U. S. A.* **89,** 353–357
7. Bazzi, H., Getz, A., Mahoney, M. G., Ishida-Yamamoto, A., Langbein, L., Wahl, J. K., III, and Christiano, A. M. (2006) *Differentiation* **74,** 129–140
8. Lundstrom, A., and Egelrud, T. (1990) *J. Invest. Dermatol.* **94,** 216–220
9. Suzuki, Y., Koyama, J., Moro, O., Horii, I., Kikuchi, K., Tanida, M., and Tagami, H. (1996) *Br. J. Dermatol.* **134,** 460–464
10. King, I. A., Tabiowo, A., and Fryer, P. R. (1987) *J. Cell Biol.* **105,** 3053–3063
11. Simon, M., Jonca, N., Guerrin, M., Haftek, M., Bernard, D., Caubet, C., Egelrud, T., Schmidt, R., and Serre, G. (2001) *J. Biol. Chem.* **276,** 20292–20299
12. Lundstrom, A., and Egelrud, T. (1988) *J. Invest. Dermatol.* **91,** 340–343
13. Borgono, C. A., Michael, I. P., and Diamandis, E. P. (2004) *Mol. Cancer Res.* **2,** 257–280
14. Brattsand, M., and Egelrud, T. (1999) *J. Biol. Chem.* **274,** 30033–30040
15. Ekholm, I. E., Brattsand, M., and Egelrud, T. (2000) *J. Invest. Dermatol.* **114,** 56–63
16. Egelrud, T., and Lundstrom, A. (1991) *Arch. Dermatol. Res.* **283,** 108–112
17. Lundstrom, A., and Egelrud, T. (1991) *Acta Dermatol. Venereol.* **71,** 471–474
18. Hansson, L., Stromqvist, M., Backman, A., Wallbrandt, P., Carlstein, A., and Egelrud, T. (1994) *J. Biol. Chem.* **269,** 19420–19426
19. Sondell, B., Thornell, L. E., Stigbrand, T., and Egelrud, T. (1994) *J. Histochem. Cytochem.* **42,** 459–465

20. Sondell, B., Thornell, L. E., and Egelrud, T. (1995) *J. Invest. Dermatol.* **104,** 819–823
21. Ishida-Yamamoto, A., Simon, M., Kishibe, M., Miyauchi, Y., Takahashi, H., Yoshida, S., O'Brien, T. J., Serre, G., and Iizuka, H. (2004) *J. Invest. Dermatol.* **122,** 1137–1144
22. Ishida-Yamamoto, A., Deraison, C., Bonnart, C., Bitoun, E., Robinson, R., O'Brien, T. J., Wakamatsu, K., Ohtsubo, S., Takahashi, H., Hashimoto, Y., Dopping-Hepenstal, P. J., McGrath, J. A., Iizuka, H., Richard, G., and Hovnanian, A. (2005) *J. Invest. Dermatol.* **124,** 360–366
23. Brattsand, M., Stefansson, K., Lundh, C., Haasum, Y., and Egelrud, T. (2005) *J. Invest. Dermatol.* **124,** 198–203
24. Caubet, C., Jonca, N., Brattsand, M., Guerrin, M., Bernard, D., Schmidt, R., Egelrud, T., Simon, M., and Serre, G. (2004) *J. Invest. Dermatol.* **122,** 1235–1244
25. Descargues, P., Deraison, C., Prost, C., Fraitag, S., Mazereeuw-Hautier, J., D'Alessio, M., Ishida-Yamamoto, A., Bodemer, C., Zambruno, G., and Hovnanian, A. (2006) *J. Invest. Dermatol.* **126,** 1622–1632
26. Komatsu, N., Takata, M., Otsuki, N., Toyama, T., Ohka, R., Takehara, K., and Saijoh, K. (2003) *J. Invest. Dermatol.* **121,** 542–549
27. Kuwae, K., Matsumoto-Miyai, K., Yoshida, S., Sadayama, T., Yoshikawa, K., Hosokawa, K., and Shiosaka, S. (2002) *Mol. Pathol.* **55,** 235–241
28. Komatsu, N., Saijoh, K., Toyama, T., Ohka, R., Otsuki, N., Hussack, G., Takehara, K., and Diamandis, E. P. (2005) *Br. J. Dermatol.* **153,** 274–281
29. Komatsu, N., Saijoh, K., Sidiropoulos, M., Tsai, B., Levesque, M. A., Elliott, M. B., Takehara, K., and Diamandis, E. P. (2005) *J. Invest. Dermatol.* **125,** 1182–1189
30. Stefansson, K., Brattsand, M., Ny, A., Glas, B., and Egelrud, T. (2006) *Biol. Chem.* **387,** 761–768
31. Komatsu, N., Takata, M., Otsuki, N., Ohka, R., Amano, O., Takehara, K., and Saijoh, K. (2002) *J. Invest. Dermatol.* **118,** 436–443
32. Descargues, P., Deraison, C., Bonnart, C., Kreft, M., Kishibe, M., Ishida-Yamamoto, A., Elias, P., Barrandon, Y., Zambruno, G., Sonnenberg, A., and Hovnanian, A. (2005) *Nat. Genet.* **37,** 56–65
33. Hachem, J. P., Wagberg, F., Schmuth, M., Crumrine, D., Lissens, W., Jayakumar, A., Houben, E., Mauro, T. M., Leonardsson, G., Brattsand, M., Egelrud, T., Roseeuw, D., Clayman, G. L., Feingold, K. R., Williams, M. L., and Elias, P. M. (2006) *J. Invest. Dermatol.* **126,** 1609–1621
34. Greene, S. L., and Muller, S. A. (1985) *J. Am. Acad. Dermatol.* **13,** 329–337
35. Chavanas, S., Bodemer, C., Rochat, A., Hamel-Teillac, D., Ali, M., Irvine, A. D., Bonafe, J. L., Wilkinson, J., Taieb, A., Barrandon, Y., Harper, J. I., de Prost, Y., and Hovnanian, A. (2000) *Nat. Genet.* **25,** 141–142
36. Sprecher, E., Chavanas, S., DiGiovanna, J. J., Amin, S., Nielsen, K., Prendiville, J. S., Silverman, R., Esterly, N. B., Spraker, M. K., Guelig, E., de Luna, M. L., Williams, M. L., Buehler, B., Siegfried, E. C., Van Maldergem, L., Pfendner, E., Bale, S. J., Uitto, J., Hovnanian, A., and Richard, G. (2001) *J. Invest. Dermatol.* **117,** 179–187
37. Magert, H. J., Standker, L., Kreutzmann, P., Zucht, H. D., Reinecke, M., Sommerhoff, C. P., Fritz, H., and Forssmann, W. G. (1999) *J. Biol. Chem.* **274,** 21499–21502
38. Bitoun, E., Micheloni, A., Lamant, L., Bonnart, C., Tartaglia-Polcini, A., Cobbold, C., Al Saati, T., Mariotti, F., Mazereeuw-Hautier, J., Boralevi, F., Hohl, D., Harper, J., Bodemer, C., D'Alessio, M., and Hovnanian, A. (2003) *Hum. Mol. Genet.* **12,** 2417–2430
39. Egelrud, T., Brattsand, M., Kreutzmann, P., Walden, M., Vitzithum, K., Marx, U. C., Forssmann, W. G., and Magert, H. J. (2005) *Br. J. Dermatol.* **153,** 1200–1203
40. Schechter, N. M., Choi, E. J., Wang, Z. M., Hanakawa, Y., Stanley, J. R., Kang, Y., Clayman, G. L., and Jayakumar, A. (2005) *Biol. Chem.* **386,** 1173–1184
41. Franzke, C. W., Baici, A., Bartels, J., Christophers, E., and Wiedow, O. (1996) *J. Biol. Chem.* **271,** 21886–21890
42. Galliano, M. F., Toulza, E., Gallinaro, H., Jonca, N., Ishida-Yamamoto, A., Serre, G., and Guerrin, M. (2006) *J. Biol. Chem.* **281,** 5780–5789
43. Laxmikanthan, G., Blaber, S. I., Bernett, M. J., Scarisbrick, I. A., Juliano, M. A., and Blaber, M. (2005) *Proteins* **58,** 802–814
44. Bernett, M. J., Blaber, S. I., Scarisbrick, I. A., Dhanarajan, P., Thompson, S. M., and Blaber, M. (2002) *J. Biol. Chem.* **277,** 24562–24570
45. Michael, I. P., Sotiropoulou, G., Pampalakis, G., Magklara, A., Ghosh, M., Wasney, G., and Diamandis, E. P. (2005) *J. Biol. Chem.* **280,** 14628–14635
46. Sotiropoulou, G., Rogakos, V., Tsetsenis, T., Pampalakis, G., Zafiropoulos, N., Simillides, G., Yiotakis, A., and Diamandis, E. P. (2003) *Oncol. Res.* **13,** 381–391
47. Felber, L. M., Borgono, C. A., Cloutier, S. M., Kundig, C., Kishi, T., Ribeiro, C. J., Jichlinski, P., Gygi, C. M., Leisinger, H. J., Diamandis, E. P., and Deperthes, D. (2005) *Biol. Chem.* **386,** 291–298
48. Jayakumar, A., Kang, Y., Henderson, Y., Mitsudo, K., Liu, X., Briggs, K., Wang, M., Frederick, M. J., El Naggar, A. K., Bebok, Z., and Clayman, G. L. (2005) *Arch. Biochem. Biophys.* **435,** 89–102
49. Jayakumar, A., Kang, Y., Mitsudo, K., Henderson, Y., Frederick, M. J., Wang, M., El Naggar, A. K., Marx, U. C., Briggs, K., and Clayman, G. L. (2004) *Protein Expr. Purif.* **35,** 93–101
50. Raghunath, M., Tontsidou, L., Oji, V., Aufenvenne, K., Schurmeyer-Horst, F., Jayakumar, A., Stander, H., Smolle, J., Clayman, G. L., and Traupe, H. (2004) *J. Invest. Dermatol.* **123,** 474–483
51. Chao, J. (2004) in *Handbook of Proteolytic Enzymes* (Barrett, A. D., Rawlings, N. D., and Woessner, J. F., eds) 2nd Ed., Vol. 2, pp. 1577–1580, Elsevier Academic Press, London
52. Magklara, A., Mellati, A. A., Wasney, G. A., Little, S. P., Sotiropoulou, G., Becker, G. W., and Diamandis, E. P. (2003) *Biochem. Biophys. Res. Commun.* **307,** 948–955
53. Kapadia, C., Yousef, G. M., Mellati, A. A., Magklara, A., Wasney, G. A., and Diamandis, E. P. (2004) *Clin. Chim. Acta* **339,** 157–167
54. Borgono, C. A., Michael, I. P., Shaw, J. L., Luo, L. Y., Ghosh, M. C., Soosaipillai, A., Grass, L., Katsaros, D., and Diamandis, E. P. (November 16, 2006) *J. Biol. Chem.* 10.1074/jbc.M608348200
55. Kreutzmann, P., Schulz, A., Standker, L., Forssmann, W. G., and Magert, H. J. (2004) *J. Chromatogr. B Analyt. Technol. Biomed. Life Sci.* **803,** 75–81
56. Rawlings, N. D., Tolle, D. P., and Barrett, A. J. (2004) *Biochem. J.* **378,** 705–716
57. Laskowski, M., Jr., and Kato, I. (1980) *Annu. Rev. Biochem.* **49,** 593–626
58. Wiedow, O., Young, J. A., Davison, M. D., and Christophers, E. (1993) *J. Invest. Dermatol.* **101,** 305–309
59. Wiedow, O., Schroder, J. M., Gregory, H., Young, J. A., and Christophers, E. (1990) *J. Biol. Chem.* **265,** 14791–14795
60. Shimomura, Y., Sato, N., Kariya, N., Takatsuka, S., and Ito, M. (2005) *Br. J. Dermatol.* **153,** 1026–1030
61. Grutter, M. G., Fendrich, G., Huber, R., and Bode, W. (1988) *EMBO J.* **7,** 345–351
62. Ying, Q. L., and Simon, S. R. (1993) *Biochemistry* **32,** 1866–1874
63. Ohlsson, K., Bjartell, A., and Lilja, H. (1995) *J. Androl.* **16,** 64–74
64. Hiemstra, P. S., Maassen, R. J., Stolk, J., Heinzel-Wieland, R., Steffens, G. J., and Dijkman, J. H. (1996) *Infect. Immun.* **64,** 4520–4524
65. Eisenberg, S. P., Hale, K. K., Heimdal, P., and Thompson, R. C. (1990) *J. Biol. Chem.* **265,** 7976–7981
66. Taggart, C. C., Lowe, G. J., Greene, C. M., Mulgrew, A. T., O'Neill, S. J., Levine, R. L., and McElvaney, N. G. (2001) *J. Biol. Chem.* **276,** 33345–33352
67. Jin, F. Y., Nathan, C., Radzioch, D., and Ding, A. (1997) *Cell* **88,** 417–426
68. Ohman, H., and Vahlquist, A. (1994) *Acta Derm. Venereol.* **74,** 375–379
69. Hanakawa, Y., Selwood, T., Woo, D., Lin, C., Schechter, N. M., and Stanley, J. R. (2003) *J. Invest. Dermatol.* **121,** 383–389
70. Hanakawa, Y., Schechter, N. M., Lin, C., Garza, L., Li, H., Yamaguchi, T., Fudaba, Y., Nishifuji, K., Sugai, M., Amagai, M., and Stanley, J. R. (2002) *J. Clin. Invest.* **110,** 53–60
71. Bieth, J. G. (1984) *Biochem. Med.* **32,** 387–397
72. Bieth, J. G. (1995) *Methods Enzymol.* **248,** 59–84
73. Magert, H. J., Kreutzmann, P., Standker, L., Walden, M., Drogemuller, K., and Forssmann, W. G. (2002) *Int. J. Biochem. Cell Biol.* **34,** 573–576
74. Ahmed, A., Kandola, P., Ziada, G., and Parenteau, N. (2001) *J. Protein Chem.* **20,** 273–278
75. Tartaglia-Polcini, A., Bonnart, C., Micheloni, A., Cianfarani, F., Andre, A., Zambruno, G., Hovnanian, A., and D'Alessio, M. (2006) *J. Invest. Dermatol.* **126,** 315–324
76. Talas, U., Dunlop, J., Khalaf, S., Leigh, I. M., and Kelsell, D. P. (2000) *J. Invest. Dermatol.* **114,** 165–170
77. Fiedler, F. (1987) *Eur. J. Biochem.* **163,** 303–312

78. Bourgeois, L., Brillard-Bourdet, M., Deperthes, D., Juliano, M. A., Juliano, L., Tremblay, R. R., Dube, J. Y., and Gauthier, F. (1997) *J. Biol. Chem.* **272,** 29590–29595
79. Chen, V. C., Chao, L., and Chao, J. (2000) *J. Biol. Chem.* **275,** 38457–38466
80. Krebs, M., Uhrin, P., Vales, A., Prendes-Garcia, M. J., Wojta, J., Geiger, M., and Binder, B. R. (1999) *J. Invest. Dermatol.* **113,** 32–37
81. Oji, V., Oji, M. E., Adamini, N., Walker, T., Aufenvenne, K., Raghunath, M., and Traupe, H. (2006) *Br. J. Dermatol.* **154,** 860–867
82. Whittock, N. V., and Bower, C. (2003) *Clin. Exp. Dermatol.* **28,** 410–415
83. Chitaev, N. A., and Troyanovsky, S. M. (1997) *J. Cell Biol.* **138,** 193–201
84. Noe, V., Fingleton, B., Jacobs, K., Crawford, H. C., Vermeulen, S., Steelant, W., Bruyneel, E., Matrisian, L. M., and Mareel, M. (2001) *J. Cell Sci.* **114,** 111–118

Enzyme Catalysis and Regulation:

A Potential Role for Multiple Tissue Kallikrein Serine Proteases in Epidermal Desquamation

Carla A. Borgoño, Iacovos P. Michael, Nahoko Komatsu, Arumugam Jayakumar, Ravi Kapadia, Gary L. Clayman, Georgia Sotiropoulou and Eleftherios P. Diamandis

J. Biol. Chem. 2007, 282:3640-3652.
doi: 10.1074/jbc.M607567200 originally published online December 11, 2006